TEMPORAL AND SPATIAL DEPENDENCY OF HIGH FREQUENCY WAVE COLLISIONS IN RAT SOMATOSENSORY CORTEX

By

Alexander Carvajal

A dissertation submitted in partial fulfillment of the requirements for the degree of

MASTER OF SCIENCE IN NEUROSCIENCE

WASHINGTON STATE UNIVERSITY
Program in Neuroscience

August 2008

To the Faculty of Washington State University:

The members of the Committee appointed to examine the dissertation of ALEXANDER CARVAJAL find it satisfactory and recommend that it be accepted.

Chair

TEMPORAL AND SPATIAL DEPENDENCY OF HIGH FREQUENCY WAVE COLLISIONS IN RAT SOMATOSENSORY CORTEX

ABSTRACT

By Alexander Carvajal, MD
Washington State University
August 2008

Chair: David Rector

Multivibrissal sensory integration may be accomplished through the interaction of interference patterns from fast oscillatory (FO) spreading waves across cortical barrels; analogous to waves in water. We studied the interference patterns of FO occurring after paired whisker stimulation and examined the relative wave amplitudes under different whisker stimulus delays and directions. We observed both supralinear and sublinear FO integration that was sensitive to 0-5 ms time delays and to the sequential order in which whiskers were stimulated. The somatosensory evoked potential (SEP) measured between the two cortical columns was not significantly affected by these short delays. Since the maximal and minimal response occurred during delay times corresponding to a FO half period, we hypothesize that wave interference and collisions are responsible for modulating the final amplitude of the spreading wave. The maximum effect occurred between barrels of the same whisker row in the rostral to caudal direction but also occurred to a lesser extent between cortical barrels of the same whisker arc. These results suggest that FOs preferentially interfere in the rostral to caudal whisker direction, which

may represent the natural flow of information as the rat whisks in its environment. FO spreading also occurred in other directions but produced less pronounced interference effects, probably related to differences in the organization of underlying circuitry and coupling.

LIST OF FIGURES

LIST OF TABLES

TABLE OF CONTENTS

Page

INTRODUCTION

Somatosensory stimulation produces a well-defined somatosensory evoked potential (SEP) recorded on the surface of the somatosensory cortex. The SEP shows a dominant frequency of ~40 Hz but also contains fast electrical oscillations (FO) with frequencies greater than 200 Hz. FOs have been recorded using electroencephalographic and magnetoencephalographic recordings in different species, including rats (Jones and Barth, 1999) and humans (Curio et al, 1994b; Hashimoto et al, 1996; Ozaki and Hashimoto, 2005). These oscillations may be involved in normal brain activity and also in brain pathologies such as seizures and movement disorders (Mochizuki et al, 1999; Rampp and Stefan, 2006). FOs have been divided into high-frequency oscillations (HFO) ranging between 200 Hz and 400 Hz and very high-frequency oscillations (VHFO) ranging between 400 Hz and 600 Hz, superimposed on the low-frequency SEP (Jones et al, 2000). In addition, previous studies have shown that fast oscillations are somatotopically organized in the somatosensory cortex, occurring in the barrel corresponding to the vibrissae stimulated, and then spreading to adjacent barrels with lower amplitude (Jones and Barth 1999). We are ultimately interested in understanding how interference patterns created by colliding waves could be used as a mechanism for sensory processing.

The anatomical and cellular basis of the FOs are not well understood, but they appear to be related to stochastic firing of action potentials within the cortical barrels (Jones et al, 2000). Cells receiving inputs from ventroposteriomedial (VPM) thalamic cells located in cortical layer IV are the first input for sensory information in a highly hierarchical cortical network. These cells include regular spiking pyramidal cells, and two types of interneurons, the fast-spiking inhibitory interneurons

(smooth cells) and the spiny stellate excitatory interneurons (Jones and Diamond, 1995; Zhu and Connors, 1999; Bruno and Simons, 2002). There is some evidence suggesting that the HFO neurogenerator may arise from activation of local cortical circuits containing regular spiking cells plus spiny stellate cells through thalamic projections. In contrast, the VHFO neurogenerator may arise from activation of fast-spiking cells (Jones et al, 2000; Ozaki and Hashimoto, 2005). However, HFOs could also be generated by subcortical high-frequency bursts from thalamic barreloids cells (Klostermann et al, 2002).

Stimulus-induced, synchronous oscillations are a characteristic feature of neuronal assembly dynamics and could play an important role in sensory processing. For example, sensory stimulation in retinal ganglion cells induce synchronized firing patterns transmitted to cells in the lateral geniculate nucleus (Neuenschwander and Singer, 1996). Synchronized firing patterns have also been shown in distant cortical regions that share the same receptive field (Bressler et al, 1993; Bruns and Eckhorn, 2004). The underlying mechanism for this synchronous activity may be the engagement of cortical networks by a temporal coherent spike wavefront generated by the stimulus and propagated through dendrodendritic connections (Rowe, 1990; Farhat et al, 1991; Eccles, 1992). Since, membrane potential oscillations are generated by external stimuli and the various synaptic steps along the sensory pathway, it is possible that these oscillations underly the spike wavefront. Various brain regions exhibiting phase locked interactions have been documented, including the visual, auditory and somatosensory cortex, mostly in the gamma-frequency band (30-100 Hz) (Fries et al, 2007), and seem to be dependent on gap junction connections between inhibitory interneurons (Singer, 1999).

Since neighboring dendrites may be connected through gap junctions (Dermietzel and Spray, 1993), it is feasible that phase synchrony between different neuronal networks on a local and large scale could be the basis for brain integration, and this synchrony could be explained by the propagation of traveling waves through gap junctions within cortical networks. Growing experimental and theoretical evidence shows that rapid neuronal activity can behave as standing and traveling waves in the visual cortex, and might be involved in scanning different stimulus attributes (Ermentrout and Kleinfeld, 2001; Lee et al, 2004; Benucci et al, 2007). Since, rapid neuronal activity can spread in a wave like fashion through gap junctions; interference patterns of these waves could account for complex sensory processing as proposed in Pribram's holonomic theory (Pribram, 1991).

To further support the importance of FOs, high-frequency electrical stimulation of subcortical brain structures (deep brain stimulation [DBS]) has been used effectively for clinical treatment in refractory neurological disorders like epilepsy, Parkinson's disease, and Tourette's Syndrome (Durand and Jensen, 2006). However, the mechanisms underlying the response of neurons to these applied high-frequency electric fields have not yet been elucidated, tempering the success of this treatment (McIntyre et al, 2007). A better understanding of FOs properties could be beneficial for the development of improved prosthetic devices.

In the present study, we hypothesize that the propagation and interference patterns of the HFO and VHFO within the somatosensory cortex will change, depending on the sequential order of whisker stimulation in the rostrocaudal (row) and ventromedial (arc) axis. Since the output of primary sensory cortex could be driven by the wave patterns appearing on the cortical surface, this could be

an important mechanism underlying the integration of information after multiwhisker stimulation. Therefore, we studied the standing wave spreading pattern after synchronous and asynchronous stimulation of two vibrissae in the same row, and in the same arc. Our aim was to determine possible supralinear or sublinear responses of the HFO and VHFO after their collision as a function of millisecond delays between two whisker stimulation.

MATERIALS AND METHODS

Surgical Preparation

Six Sprague-Dawley rats were anesthetized to surgical levels using intramuscular injections of ketamine HCl (100 mg/kg) and xylazine (5 mg/kg) and were secured in a stereotaxic frame. The unilateral (right hemisphere) parietal-temporal cortex was exposed and the bone removed 2 mm anterior to lambda, 2 mm lateral to the sagital suture, 2 mm lateral to the temporal ridge and 1 mm posterior to bregma (Fig. 1). The exposed area was regularly moistened with physiological saline solution, and body temperature was maintained with a regulated heating pad. Supplemental doses of ketamine and xylazine were injected as required to maintain a level of anesthesia such that the pinch reflex and the corneal reflex could not be elicited. Animals were euthanized by an intraperitoneal (IP) injection of sodium pentobarbital at the end of the experiment. Surgical procedures were performed in accordance with the Guide for Care and Use of Laboratory Animals and were approved by the Washington State University Animal Care and Use Committee.

Electrophysiological Recordings

A 5x5 mm 64 multi-electrode array (Fig. 1E) was placed over the somatosensory cortex to record surface field potentials during whisker stimulation. Initially the dura was left intact to localize the barrels, then the dura was removed to obtain better signals by reducing current spread through the dural tissue. The animals were instrumented with one screw electrode over the frontal lobe to record electroencephalogram EEG and with a reference screw electrode over the occipital lobe. Subcutaneous needle electrodes were placed on the thoracic cage to record electrochardiogram EKG and respiration. All signals were amplified (x 1000), filtered using butterworth filters (0.1 Hz – 3

KHz), and digitized at 20 KHz (Rector et al, 2001).

Stimulation

Cortical barrel mapping was performed by whisker stimulation in a 1-2 s random inter-stimulus interval (ISI), by means of a laboratory-made solenoid twitcher that moved 1 mm/2 ms (0.5 m/s). Four whisker barrels were located under the electrode array, then two whiskers of the same row and two whiskers of the same arc were stimulated with different delays ranging between 0 ms to 4.5 ms. The row-wise delay stimulation was applied in a caudal to rostral direction and vice versa. For the arc-wise stimulation, the delay stimulation was applied in a dorsal to ventral direction and vice versa.

Data Collection and Analysis

Responses were computed by averaging multiple individual trials (n = 50) during whisker stimulation. P1 was defined as the largest SEP peak that occurred ~15 to 20 ms after the stimulus, and N1 was defined as the largest deflection that occurred ~20 to 25 ms after stimulus (Di and Barth, 1991).

Evoked responses were band-pass filtered in two frequency ranges (200 to 400 Hz; 400 to 600 Hz) using an IIRC software based butterworth filter, with correction for backward and forward calculations. HFO and VHFO amplitudes were computed taking the highest point of the envelope of the plot that occurred ~15 to 20 ms after the stimulus. Statistical analysis was performed on the HFO and VHFO response maximal peak amplitude. One or two factor ANOVA, followed by the Holm-Sidak method when appropriate and Student's paired *t*-test for post hoc multiple comparisons were carried out for data analysis. For most comparisons a Kolmogorov-Smirnov test for a normal

distribution indicated that a parametric test could be used. Due to the small sample size, we chose a significance value of $p = < 0.05$ to determine difference between delays.

RESULTS

The evoked response of the barrel field corresponding to single whisker stimulation c0, c2, c1 and d1 were consistently located under the multi-electrode array in each rat (Fig 2). In order to compare the values between animals when two whiskers were stimulated, peak amplitude values were normalized across trials using the value obtained during synchronous whisker stimulation with no delay. We found sublinear summation in the SEP peak amplitude. [c2+c0: 55.16 % $^{+}_{-}$ 9.52 ($p < 0.001$) ; c0+c2: 66.81 % $^{+}_{-}$ 11.34 ($p < 0.001$); c1+d1: 58.59 $^{+}_{-}$ 6.12 ($p < 0.001$); d1+c1: 41.79 % $^{+}_{-}$ 19.17 ($p < 0.001$)], and for the most part did not change significantly with different delays. HFO and VHFO amplitudes had different sensitivity to stimulus delays, two way ANOVA analysis with delay and type of wave as factors showed significant differences in sensitivity to stimulus delays in both the rostrocaudal axis (Fig. 3) and the dorsoventral axis (see Table 1, Table 2, Fig 4 and Fig 5).

Rostrocaudal axis - SEP

The SEP voltage peak amplitude, elicited after stimulating whiskers c0 and c2 simultaneously and at different delays, showed no significant difference when they were stimulated in a *rostral to caudal* sequence, nor when they were stimulated in a *caudal to rostral* sequence [(ANOVA ($F(9,50) = 0.616$ $p = 0.778$); (ANOVA ($F(9,50) = 0.353$ $p = 0.952$); (see table 1and Fig. 4A)].

Rostrocaudal axis - HFO

The HFO (200 to 400) voltage peak amplitude, elicited after simultaneously stimulating whiskers

c0 and c2 in a *rostral to caudal* sequence and at different delays, showed significant differences [(ANOVA ($F(9,50) = 3.170$ $p = 0.004$)]. Post-hoc analysis using a paired *t*-test showed a significant amplitude increase after asynchronous stimulation at 0.6 ms delay when compared to synchronous stimulation and a significant amplitude decreases at 3.6 ms delay. The HFO voltage peak amplitude elicited after stimulating whiskers c0 and c2 in the *caudal to rostral* sequence simultaneously and at different delays showed significant decrease in amplitude with increasing delays compared with synchronous stimulation [(ANOVA ($F(9,50) = 2.276$ $p = 0.032$); (see Table 1)]. Two way ANOVA analysis with delay and direction as factors showed significant HFO voltage peak amplitude differences [$F(19,100) = 5.711$ $p = 0.019$], at 0.6 ms [$p= 0.03$], suggesting that the interference patterns depended on the stimulation sequence (Fig. 4B).

Rostrocaudal axis - VHFO

The ANOVA and post-hoc paired *t*-test analysis of the VHFO (400-600 Hz) voltage peak amplitude elicited after simultaneously stimulating whiskers c0 and c2 in a *rostral to caudal* sequence and at different delays showed a significant amplitude increase after asynchronous stimulation at 0.6 ms compared to synchronous stimulation and showed a significant amplitude decrease at 1.5, 2.4, 2.7, 3.3 and 3.6 ms delay [($F(9,50) = 7.998$ $p = <0.000$); (see Table 1)]. We observed a significant recovery of the amplitude at 2.4 ms suggesting a cyclical phase-sensitive enhancement or attenuation of VHFOs with a half-period of 1 msec aprox (see Table 1 and Fig. 4C). The VHFO voltage peak amplitude, elicited after simultaneously stimulating whiskers c0 and c2 in a *rostral to caudal* sequence and at different delays showed no significant differences, suggesting a

different behavior of VHFO interference [(ANOVA ($F(9,50) = 0.543$ $p = 0.836$); (see Table 1)]. Two way ANOVA analysis with delay and direction as factors, showed significant VHFO voltage peak amplitude differences [$F(9,100) = 7.658$ $p = 0.007$], at 3.6 ms delay [$p= 0.03$]. These results again suggest a different interference pattern depending on the stimulation sequence (Fig. 4C).

Dorsoventral axis - SEP

The SEP voltage peak amplitude elicited after stimulating whiskers c1 and d1 simultaneously and at different delays showed no significant difference when they were stimulated in a *dorsal to ventral* sequence (except for the two longest delays), nor when they were stimulated in a *ventral to dorsal* sequence [(ANOVA ($F(9,50) = 1.478$ $p = 0.182$); (see Table 2 and Fig. 5A)].

Dorsoventral axis - HFO

The ANOVA and post-hoc paired *t*-test analysis of the HFO voltage peak amplitude (200-400 Hz) elicited after stimulating whiskers c1 and d1 in the *dorsal to ventral* sequence simultaneously and at different delays showed showed a significant decrease after asynchronous stimulation with delays at 3.3 ms and 4.2 ms [($F(9,50) = 2.445$ $p = 0.022$); (see Table 2)]. After stimulating whiskers c1 and d1 in the *ventral to dorsal* direction simultaneously and at different delays we found a significant amplitude decrease with increasing delays, suggesting the existence of interfering patterns also after paired arc whisker stimulation [(ANOVA ($F(9,50) = 2.142$ $p = 0.043$); (see Table 2)]. Two way ANOVA analysis with delay and direction as factors showed a significant HFO voltage peak amplitude differences [$F(19,100) = 20.424$ $p = <0.001$], at 0.9 ms delay [$p= 0.01$], 2.1 ms delay [$p=$

0.001] and 3.9 ms delay [p= 0.038]. As with the rostrocaudal axis, we found a dependence on the stimulation sequence on the generation of interference patterns (Fig. 5B), however supralinear integration did not occur in the dorsoventral axis

Dorsoventral axis - VHFO

The VHFO voltage peak (400-600 Hz) elicited after stimulating whiskers c1 and d1 in either sequence simultaneously and at different delays showed no significant difference [(ANOVA ($F(9,50) = 0.307$ $p = 0.969$)]. Two way ANOVA analysis with delay and direction as factors showed no significant difference [$F(19,100) = 0.079$ $p = 0.781$]. Taken together, these results suggest that there is no significant interference pattern for the VHFOs in the dorsoventral axis (Fig. 5C).

Spatial Patterns of Wave Interaction

We assessed the cortical spatial patterns of wave interaction after multiwhisker stimulation by reconstructing the spatiotemporal FO spread using color-coded maps that represent the magnitude of cortical barrel activation a cross space and time. Figure 6 depicts a typical sequence during single whisker stimulation of c0 and c2 with this analysis in which. Induced FO responses reached a maximum amplitude beneath the corresponding barrel for each whisker, then spread to adjacent barrels in different directions. The same pattern was observed for both the positive and the negative FO inflection. When two whiskers were stimulated with different delays, the FOs interference patterns increased their complexity, especially at 0.6 ms delay (Fig. 7 Top panel). At 1.5 ms (Fig. 7 middle panel) we observed a lower amplitude, lower complexity and less spread in the interference

pattern. At 2.4 ms (Fig. 7 lower panel), the amplitude, complexity and wider spread activity recovered.

DISCUSSION

We found significant interference pattern differences for HFOs and VHFOs, that were dependent on time delays and the sequence direction of stimulation. Our results suggest an important role for FO interference patterns in extracting relevant information from multiple-whisker stimulations at the millisecond level. Feature extraction could occur through phase locked interactions between different neuronal assemblies and the spreading and interference of these interactions as waves. Since spreading waves have a preferential interference pattern in the rostral to caudal direction, our data also indicate a specific connectivity within the network, and suggest that gap junction connections may join dendrites in a specific anatomical pattern as dictated by normal whisker stimulation.

Somatosensory Evoked Potential

In agreement with earlier results, the SEP showed a higher amplitude after simultaneous stimulation of whiskers c2 and c0, c1 and d1 than any single response (Di and Barth, 1991) At short delays, the SEP during simultaneous stimulation of two whiskers was smaller than the linear sum of individual stimulation, suggesting a sublinear integration of the slow-wave (Simons, 1985; Mirabella et al, 2001, Civillico and Contreras, 2006), and might be related to sensory integration (Simons, 1985; Ghazanfar and Nicolelis 1997; Shimegi et al, 1999). This was especially true for the dorsal to ventral sequence of stimulation with the longest delays. In contrast to our results, some reports show supralinear integration at short delays (<10 ms) (Ghazanfar and Nicolelis, 1997;

Shimegi et al, 1999, Ego-Stengel et al, 2004, Rodgers et al, 2006). These differences could be based on several factors including the angle of hair deflection, the particular combination of whiskers stimulated, the number of whiskers stimulated, and the cortical layer studied. Supralinear responses were usually found when more than 2 whiskers were stimulated (Ghazanfar and Nicolelis, 1997; Rodgers et al, 2006), while, sublinear responses were shown in some studies with stimulation of just two whiskers (as in this study) (Simons, 1985; Mirabella et al, 2001; Civillico and Contreras, 2006). Shimegi et al, (1999) observed supralinear integration using two whisker stimulation, but used adjacent whiskers, which might account for the differences to those presented here. Since the spatial resolution of our array was not fine enough to map changes between adjacent barrels, we stimulated non-adjacent whiskers in order to record signals between barrels where spatial overlap occurs, and allowing better images of interference patterns. Additionally, the present study used surface recordings, thus we cannot address the specific interactions that might occur at different layers. For example, supralinear neuronal responses were observed using single unit recordings at deeper levels (Ghazanfar and Nicolelis, 1997; Shimegi et al, 1999). Indeed, our results were similar to those of Civillico and Contreras, (2006) in which voltage sensitive dyes were used to measure surface potentials.

Since the SEP measured at the surface was not sensitive to short time delays nor to the sequential order in which whiskers were stimulated, our results suggest that the early SEP components did not exhibit a short latency submillisecond phase sensitivity. Others observed that the sublinearity index of the SEP activity increases significantly only after 7 ms of the stimulus onset (Mirabella et al, 2001), thus, it is plausible that sensory integration occurs later in time for the SEP compared with FOs. Indeed, the later SEP components (N1 and P2), believed to be the primary period of sensory

integration occur 15 ms after the stimulus (Simons, 1985). These later components may be related to the activation of distal apical dendrites of pyramidal cells in both layers (Di et al, 1990) involving circuits within the cortical column (Armstrong-James et al, 1991).

In contrast, we believe that FOs may provide a faster and more sensitive mechanism for spatial and temporal integration. FOs are superimposed on the early component of the SEP (P1)(Jones et al, 2000; Barth, 2003), and the early SEP component is believed to create a brief moment of intra- and interbarrel excitation through the activation of proximal apical dendrites of supragranular (Di et al. 1990) and infragranular (Staba et al. 2004) pyramidal cells perhaps through a thalamocortical volley (Armstrong-James et al, 1993). This period of excitation may be responsible for elevating the membrane potential of the column, therefore making it more sensitive to small membrane potential fluctuations generated by FOs. In addition, the SEP may play a different role than FOs in sensory integration. For example, the angular tunning of SEP is wider compared to that for FOs (Rodgers et al, 2006). Since FOs are higher in frequency than the basic components of the SEP, they may contain more information to achieve higher spatial contrast with higher time resolution.

Fast Oscillations

Our results indicate that FOs spread within the somatosensory cortex after sensory input, resulting in collisions during multivibrissal stimulation. These collisions were sensitive to time delays and to the sequential order in which whiskers were stimulated.

HFO and VHFO collision patterns were different, suggesting unique properties in the anatomical

connections of the underlying circuitry. Regular Spiking Units (RSUs) may be responsible for HFO generation, have small receptive fields, and are strongly inhibited by adjacent whisker deflections. Fast Spiking Units (FSUs) may generate the VHFOs, have strong adjacent whisker excitatory responses, and relatively weak inhibitory surrounds (Simons, 1995). Thalamocortical projections could also modify the FO collision patterns, while they predominantly innervate one barrel, they also send projections to adjacent barrels (Senft and Woolsey, 1991; Kim and Ebner, 1999). Indeed the thalamus may be involved in generating FOs in humans (Gobbele et al, 1999) and in piglets (Ikeda et al, 2002).

In spite of evidence for thalamic involvement in FO generation, two independent mechanisms may exist. FOs could still be generated when the thalamic ventrobasal complex was lesioned, and were abolished with intact thalamic input while the cortex was cooled (Staba et al, 2003). Activity within the thalamocortical loop may reverberate within milliseconds to the somatosensory cortex and contribute to the observed FOs (Ghazanfar and Nicolelis, 1997). Additionally, the thalamus may serve as a trigger for phase locked synchronization of neural assemblies on a local and large scale through direct (monosynaptic) (Shumikhina and Molotchnikoffor, 1999) or indirect (polysynaptic) (Cardin et al, 2005) connections. Since the thalamus serves as a relay for a wide distribution of sensory input, the thalamus could participate in sensory integration, specially for the HFO component of the wave interference. Since the VHFO may be primarily generated within the cortical column, the thalamus may be less involved in generating waves at this fequency (Jones et al, 2000).

Non linearity and Time dependence

Earlier studies have demonstrated that time dependent interactions between FOs produce a nonlinear summation response, probably related with a phase synchrony of the fast oscillatory burst with additive and suppressive effects depending on interval interstimulus increase at the millisecond level (Jones and Barth, 1999; Barth, 2003). Since, no significant changes were observed in the SEP amplitude at short interval delays, it is possible that the underlying mechanisms for non-linear interaction are different for SEP, HFOs and VHFOs. Sublinear and supralinear effects can be explained for HFOs and VHFOs by simple summation and cancellation through wave interference. In contrast, both early supralinear and later sublinear SEP interaction may be accomplished through feedforward inhibition, where a brief window of excitability is followed by inhibitory suppression, perhaps due to monosynaptic thalamocortical excitatory input to pyramidal cells plus and tandem input to inhibitory interneurons (Gabernet et al. 2005; Sun et al. 2006).

Since the peak FO amplitude recovers with a half period of the FO wave, and is lower as the delay increases, it may be possible that the wave interference process observed is shaped by inhibitory processes within the circuitry. Indeed, sublinear integration may play a role in spatial contrast enhancement within the receptive field. During whisking, rats stimulate many whiskers at the same time, the overall sublinear summation may suppress the less meaningful responses from adjacent whiskers leaving only the more meaningful responses from principal whiskers (Simmons, 1985; Brumberg et al, 1996). Spatial contrast may be achieved through feedforward inhibition within sublinear integration of SEP components (Gabernet et al. 2005; Sun et al. 2006). However, FO wave collisions can also achieve spatial contrast with higher time resolution.

Direction Selectivity

The results of this study also showed that FO amplitude depended on the order of whisker stimulation, suggesting that gap junction connections between barrels exhibit a specific anatomical organization. Changes in FO integration occurred after stimulating whiskers in both the rostrocaudal and the dorsoventral axis, suggesting standing waves propagate and collide between both rows and arcs, but with different efficiency. Since both supralinear and sublinear effects in both HFOs and VHFOs occurred when whiskers were stimulated in the rostral to caudal sequence and only sublinear effects for HFOs occured for other sequences of stimulation. These results suggest specific connectivity and physiological properties within the barrel network, that prefer the rostral to caudal direction. Indeed, biased connectivity in the row direction appears in both the supra- and infragranular layers (Bernardo et al, 1990; Hoeflinger et al, 1995). Additionally, there is preference for activity in the rostral direction for RSUs, but not for FSUs (Simons, 1985; Andermann and Moore, 2006), implying somatotopically organized motion direction maps in the somatosensory cortex. These maps might be related to the spatial contrast enhancement after multiwhisker stimulation. Single unit recordings have also shown neuronal network activation after deflecting a whisker in a specific direction followed by non–direction-specific inhibitory interactions (Kida et al, 2005).

There is an anatomical basis for specific connectivity from axon projection patterns to adjacent barrels (Lorente de No, 1992), in both supragranular and infragranular layers (Kim and Ebner, 1999). However, chemical synaptic connections are unlikely to be involved in the propagation of

FOs because the application of GABA in the cortical barrels does not affect the generation of FOs (Staba et al, 2004). The application of halothane, (a gap junction blocker), does affect the generation of FOs, suggesting electrical coupling may participate in FO interaction (Staba et al, 2004). Evidence supporting electrical coupling of both barrels from the same row and the same arc arise from anatomical and physiological studies showing distal gap junction connectivity between neighboring barrels (Bernardo et al. 1990; Kleinfeld and Delaney 1996; Gibson et al, 2005), and between distal dendritic segments of GABAergic interneurons (Fukuda and Kosaka, 2003; Fukuda et al, 2006).

Perception, Learning and Consciousness

While neural integration may be the basis for perception, learning and consciousness (Tononi and Edelman, 1998), the mechanisms and locations for this integration are unclear. Some authors believe that associative areas manage sensory integration through divergent and convergent pathways, by parsing sensory information and extracting specific incoming features (Van Hoesen, 1993). For example, electrophysiological data indicate that the ventral intraparietal area (VIP) is involved in multisensory analysis of stimulus motion. The VIP area contains neurons that respond to visual stimulation and tactile stimulation and perhaps encode multiple spatial representations. (Duhamel et al, 1998). Others favor the hypothesis that local network assemblies provide the basis for integration through phase locked spiking activity (Varela et al, 2001). For example, studies of visual binding indicate that processing in the visual system is fragmented, so the various attributes of an object such as color, texture, location, motion, and edges are processed in separate brain regions and then brought together in a unified representation of the object through synchronization

(Roskies, 1999).

FO spreading that follows multivibrissal stimulation may contain information about both the time and location of sensory information (Jones and Barth, 1999). Interference of the complex FO waves may lead to a complex pattern of activity on the somatosensory cortical surface of and represent the sensory experience as a hologram. The integration of adjacent networks, in our study, may rely on phase locked spread of FOs within the cortical barrels through GAP junctions (Galarreta and Hestrin, 1999, Amitai et al, 2002), and create a substrate on which neural assemblies can interpret and respond to sensory input based on the location of peaks and valleys within the interference patterns. Within the olfactory system of insects, disturbing the synchronized pattern of cell assemblies showed a deleterious effect of on an odor discriminative task, and provides direct behavioral evidence for the role synchronized of neuronal-assemblies in sensory processing (Stopfer et al, 1997). Phase synchronization in cortical regions is only important during sensory processing but also during cognitive, motor tasks (Fries et al, 2007), Additionally, NREM sleep exhibits a slow activity (<1 hz) that behaves as a traveling wave and may have a role in synaptic plasticity (Massimini et al, 2004). We believe that studying traveling wave properties and how they are generated will be an important step in understanding the underlying mechanisms of complex sensory processing, and other brain functions.

In conclusion, sensory input generates FOs that spread across the somatosensory cortex, resulting in phase locked interference patterns that might be important for integrating and processing incoming information with high temporal and spatial resolution. Depending on the extent of gap junction connections across the brain, these results suggest that complex spreading wave patterns

could underlie synchronization of neural assemblies across the cortex, where interference patterns are functional representations of the sensory input as well as the cortical response. The summation and cancellation of waves within the interference pattern at each point in time and space may underlie the conscious interpretation of sensory input, and provide patterned output responses to the experience.

BIBLIOGRAPHY

Amitai Y, Gibson JR, Beierlein M, Patrick SL, Ho AM, Connors BW, and Golomb D. The Spatial Dimensions of Electrically Coupled Networks of Interneurons in the Neocortex. *J Neurosci* 22: 4142-52, 2002.

Andermann ML, and Moore CI. A Somatotopic Map of Vibrissa Motion Direction within a Barrel Column. *Nat Neurosci* 9: 543 – 551, 2006.

Armstrong-James M, and Callahan CA. Thalamo-Cortical Processing of Vibrissal Information in the Rat. II. Spatiotemporal Convergence in the Thalamic Ventroposterior Medial Nucleus (VPm) and its Relevance to Generation of Receptive Fields of S1 Cortical "Barrel" Neurones. *J Comp Neurol* 303: 211-24, 1991.

Armstrong-James M, Welker E and Callahan CA. The Contribution of NMDA and non-NMDA Receptors to Fast and Slow Transmission of Sensory Information in the Rat SI Barrel Cortex. *J Neurosci* 13: 2149-60, 1993.

Barth DS. Submillisecond Synchronization of Fast Electrical Oscillations in Neocortex. *J Neurosci* 23: 2502–2510, 2003.

Benucci A, Frazor RA and Carandini M. Standing Waves and Traveling Waves Distinguish Two Circuits in Visual Cortex. *Neuron* 55: 103-17, 2007.

Bernardo KL, McCasland JS, Woosley TA, and Strominger RN. Local Intra- and Interlaminar Connections in Mouse Barrel Cortex. *J Comp Neurol* 291: 231-255, 1990.

Bressler SL, Coppola R, and Nakamura R. Episodic Multiregional Cortical Coherence at Multiple Frequencies During Visual Task Performance. *Nature* 366: 153-6, 1993.

Brumberg JC, Pinto DJ and Simons DJ. Spatial Gradients and Inhibitory Summation in the Rat

Whisker Barrel System. *J Neurophysiol* 76: 130-140, 1996.

Bruno RM and Simons DJ. Feedforward Mechanisms of Excitatory and Inhibitory Cortical Receptive Fields. *J Neurosci* 22: 10966–10975, 2002.

Bruns A, and Eckhorn R. Task-Related Coupling from High- to Low-Frequency Signals Among Visual Cortical Areas in Human Subdural Recordings. *Int J Psychophysiol* 51: 97-116, 2004.

Cardin JA, Palmer LA, and Contreras D. Stimulus-dependent gamma (30-50 Hz) oscillations in simple and complex fast rhythmic bursting cells in primary visual cortex. *J Neurosci* 25: 5339-50, 2005.

Civillico EF and Contreras D. Integration of Evoked Responses in Supragranular Cortex Studied with Optical Recordings in Vivo. *J Neurophysiol* 96: 336-51, 2006.

Curio G, Mackert BM, Burghoff M, Koetitz R, Abraham-Fuchs K, and Härer W. Localization of Evoked Neuromagnetic 600 Hz Activity in the Cerebral Somatosensory System. *EEG Clin Neurophysiol*. 91: 483-487, 1994b.

Dermietzel R and Spray D.C. Gap Junctions in the Brain: Where, What type, How Many and Why?. *Trends Neurosci* 16: 186–192, 1993.

Di S, Baumgartner C, and Barth DS. Laminar Analysis of Extracellular Field Potentials in Rat Vibrissa/Barrel Cortex. *J Neurophysiol* 63: 832-40, 1990.

Di S and Barth DS. Topographic Analysis of Field Potentials in Rat Vibrissa/Barrel Cortex. *Brain Research* 546: 106-112, 1991.

Duhamel JR, Colby CL, and Goldberg ME. Ventral Intraparietal Area of the Macaque: Congruent Visual and Somatic Response Properties. *J Neurophysiol* 79:126-36, 1998.

Durand DM, Jensen A, and Bikson M. Suppression of Neural Activity with High Frequency

Stimulation. *Conf Proc IEEE Eng Med Biol Soc* 1:1624-5, 2006.

Eccles JC. Evolution of Consciousness. *Proc. Natl. Acad. Sci. U. S. A.* 89: 7320–7324, 1992.

Ego-Stengel V, Mello e Souza T, Jacob V, and Shulz DE. Spatiotemporal Characteristics of Neuronal Sensory Integration in the Barrel Cortex of the Rat. *J Neurophysiol* 93: 1450–1467, 2005.

Ermentrout BG and Kleinfeld D. Traveling Electrical Waves in Cortex Insights from Phase Dynamics and Speculation on a Computational Role. *Neuron* 29: 33-44, 2001.

Farhat NH, Eldefrawy M, and Lin SY. A Bifurcation Model of Neuronal Spike Train Patterns: A Nonlinerar Dynamic Systems Approach. Origins: Brain and Self Organization, pp 396-433. Pribram KH, Lawrence Erlbraum Associates, 1994

Fries P, Nikolić D, and Singer W. The Gamma Cycle. *Trends in Neurosci* 30: 309-316, 2007.

Fukuda T and Kosaka T. Ultrastructural study of gap junctions between dendrites of parvalbumin-containing GABAergic neurons in various neocortical areas of the adult rat. *Neuroscience* 120: 5–20, 2003.

Fukuda T, Kosaka T, Singer W, and Galuske RA. Gap Junctions Among Dendrites of Cortical GABAergic Neurons Establish a Dense and Widespread Intercolumnar Network. *J Neurosci* 26: 3434-3443, 2006.

Gabernet L, Jadhav SP, Feldman DE, Carandini M, and Scanziani M. Somatosensory Integration Controlled by Dynamic Thalamocortical Feedforward Inhibition. *Neuron* 48: 315–327, 2005.

Galarreta M, and Hestrin S. A Network of Fast-Spiking Cells in the Neocortex Connected by Electrical Synapses. *Nature* 402: 72-5, 1999.

Ghazanfar AA and Nicolelis ML. Nonlinear Processing of Tactile Information in the

Thalamocortical Loop. *J Neurophysiol* 78: 506-510, 1997.

Gibson JR, Beierlein M, and Connors BW. Functional Properties of Electrical Synapses Between Inhibitory Interneurons of Neocortical Layer 4. *J Neurophysiol* 93:467–480, 2005.

Gobbelé R, Buchner H, Scherg M, Curio G. Stability of High-Frequency (600 Hz) Components in Human Somatosensory Evoked Potentials under Variation of Stimulus Rate--Evidence for a Thalamic Origin. *Clin Neurophysiol* 110: 1659-63, 1999.

Gobbelé R, Waberski TD, Simon H, Peters E, Klostermann F, Curio G, Buchner H. Different Origins of Low- and High-Frequency Components (600 Hz) of Human Somatosensory Evoked Potentials. *Clin Neurophysiol* 115: 927-37, 2004.

Hashimoto I, Mashiko T, and Imada T. Somatic Evoked High-Frequency Magnetic Oscillations Reflect Activity of Inhibitory Interneurons in the Human Somatosensory Cortex. *EEG Clin Neurophysiol* 100: 189– 203, 1996.

Hoeflinger BF, Bennett-Clarke CA, Chiaia NL, Killackey HP, and Rhoades RW. Patterning of local intracortical projections within the vibrissae representation of rat primary somatosensory cortex. *J Comp Neurol* 354:551–563.1995

Jones MS and Barth DS. Spatiotemporal Organization of Fast (>200 Hz) Electrical Oscillations in Rat Vibrissa/Barrel Cortex. *J Neurophysiol* 82: 1599-1609, 1999.

Jones MS, MacDonald KD, Choi BJ, Dudek FE, and Barth DS. Intracellular Correlates of Fast (>200 Hz) Electrical Oscillations in Rat Somatosensory Cortex. *J Neurophysiol* 84: 1505-1518, 2000.

Ikeda H, Leyba L, Bartolo A, Wang Y, and Okada YC. Synchronized Spikes of Thalamocortical Axonal Terminals and Cortical Neurons are Detectable Outside the Pig Brain with MEG. *J*

Neurophysiol 87: 626-30, 2002.

Kida H, Shimegi S and Sato H. Similarity of Direction Tuning Among Responses to Stimulation of Different Whiskers in Neurons of Rat Barrel Cortex. *J Neurophysiol* 94: 2004-2018, 2005.

Kim U and Ebner FF. Barrels and Septa: Separate Circuits in Rat Barrels Field Cortex. *J Comp Neurol* 408: 489-505, 1999.

Kleinfeld, D, Delaney, K. Distributed Representation of Vibrissa Movement in the Upper Layers of Somatosensory Cortex Revealed with Voltage-Sensitive Dyes. *J Comp Neurol* 375: 89-108, 1996.

Klostermann F, Gobbele R, Buchner H, and Curio G. Intrathalamic Non-Propagating Generators of High-Frequency (1000 Hz) Somatosensory Evoked Potential (SEP) bursts Recorded Subcortically in Man. *Clin Neurophysiol* 113: 1001-5, 2002.

Lee SH, Blake R, and Heeger DJ. Traveling Waves of Activity in Primary Visual Cortex during Binocular Rivalry. *Nat Neurosci* 8: 22 – 23, 2004.

Lorente de Nó R. The Cerebral Cortex of the Mouse (A First Contribution--the "Acoustic" Cortex). *Somatosens Mot Res* 9: 3-36, 1992.

Massimini M, Huber R, Ferrarelli F, Hill S and Tononi G. The Sleep Slow Oscillation as a Traveling Wave. *J Neurosci* 24: 6862-6870, 2004.

McIntyre CC, Miocinovic S, and Butson CR. Computational Analysis of Deep Brain Stimulation. *Expert Rev Med Devices* 4: 615-22, 2007.

Mirabella G, Battiston S, and Diamond ME. Integration of Multiple-Whisker Inputs in Rat Somatosensory Cortex. *Cereb Cortex* 11: 164-170, 2001.

Mochizuki H, Ugawa Y, Machii K, Terao Y, Hanajima R, Furubayashi T, Uesugi H, and

Kanazawa I. Somatosensory Evoked High-Frequency Oscillation in Parkinson's Disease and Myoclonus Epilepsy. *Clin Neurophysiol* 110: 185-91, 1999.

Neuenschwander S and Singer W. Long-Range Synchronization of Oscillatory Light Responses in the Cat Retina and Lateral Geniculate Nucleus. *Nature* 379: 728-733, 1996.

Ozaki I and Hashimoto I. Neural Mechanisms of the Ultrafast Activities. *Clin EEG Neurosci* 36: 271-7, 2005.

Pribram KH. Brain and Perception, Lawrence Erlbaum Associates. 1991.

Rampp S and Stefan H. Fast Activity as a Surrogate Marker of Epileptic Network Function?. *Clin Neurophysiol* 117: 2111–2117, 2006.

Rector DM and George JS. Continous Image and Electrophysiological Recording with Real-Time Processing and Control. *Methods* 25: 151-163, 2001.

Rodgers KM, Benison AM, and Barth DS. Two-Dimensional Coincidence Detection in the Vibrissa/Barrel. Field *J Neurophysiol* 96: 1981-1990, 2006.

Roskies AL. The Binding Problem. *Neuron*, 24: 95-104, 999.

Rowe M. Impulse Patterning in Central Neurons for Vibrotactile Coding. Information Processing in the Mammalian Auditory and Tactile Systems. M Rowe and L Aitken, eds pp. 111-115. Wiley-Liss, 1990.

Senft SL and Woolsey TA. Mouse Barrel Cortex Viewed as Dirichlet Domains. *Cereb Cortex* 1: 348-63, 1991.

Shimegi S, Ichikawa T, Akasaki T, and Sato H. Temporal Characteristics of Response Integration Evoked by Multiple Whisker Stimulations in the Barrel Cortex of Rats. *J Neurosci* 19: 10164–10175, 1999.

Shumikina S and Molotchnikoff S. Pulvinar Participates in Synchronizing Neural Assemblies in the Visual Cortex, in Cats. Neuroscience letters 272: 135-139, 1999.

Simons DJ. Temporal and Spatial Integration in the Rat SI Vibrissa Cortex. *J Neurophysiol* 54: 615–635, 1985.

Simons DJ. Cerebral Cortex: Volume 11 [The Barrel Cortex of Rodents] edited by Jones EG and Diamond IT. Plenum Press, 1995.

Singer W. Neuronal Synchrony: A Versatile Code for the Definition of Relations?. *Neuron* 24: 111–125, 1999.

Staba RJ, Brett-Green B, Paulsen M, and Barth DS. Effects of Ventrobasal Lesion and Cortical Cooling on Fast Oscillations (>200 Hz) in Rat Somatosensory Cortex. *J Neurophysiol* 89: 2380–2388, 2003.

Staba RJ, Bergmann PC, Barth DS. Dissociation of Slow Waves and Fast Oscillations Above 200 Hz during GABA Application in Rat Somatosensory Cortex. *J Physiol*. 561: 205–214, 2004.

Stopfer M, Bhagavan S, Smith BH, and Laurent G. Impaired Odour Discrimination on Desynchronization of Odour-Encoding Neural Assemblies. *Nature* 390:70-4, 1997.

Sun QQ, Huguenard JR, and Prince DA. Barrel Cortex Microcircuits: Thalamocortical Feedforward Inhibition in Spiny Stellate Cells is Mediated by a Small Number of Fast-Spiking Interneurons. *J Neurosci* 26: 1219–1230, 2006.

Van Hoesen GW. The Modern Concept of Association Cortex. *Curr Opin Neurobiol* 3: 150-154, 1993.

Varela F, Lachaux JP, Rodriguez E, and Martinerie J. The Brainweb: Phase Synchronization and Large-Scale Integration. *Nat Rev Neurosci* 2: 229-39, 2001.

Zhu JJ and Connors BW. Intrinsic Firing Patterns and Whisker-Evoked Synaptic Responses of Neurons in the Rat Barrel Cortex. *J Neurophysiol* 81: 1171-1183,1999.

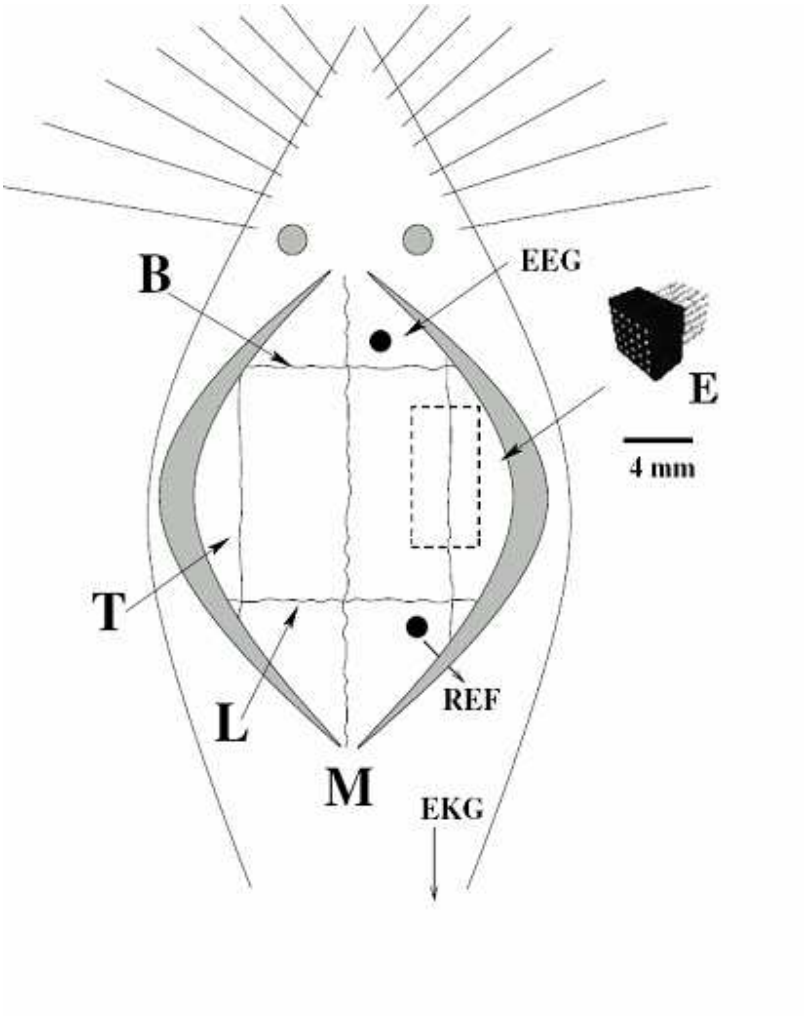
B
EEG
E
4 mm
T
L
REF
M
EKG

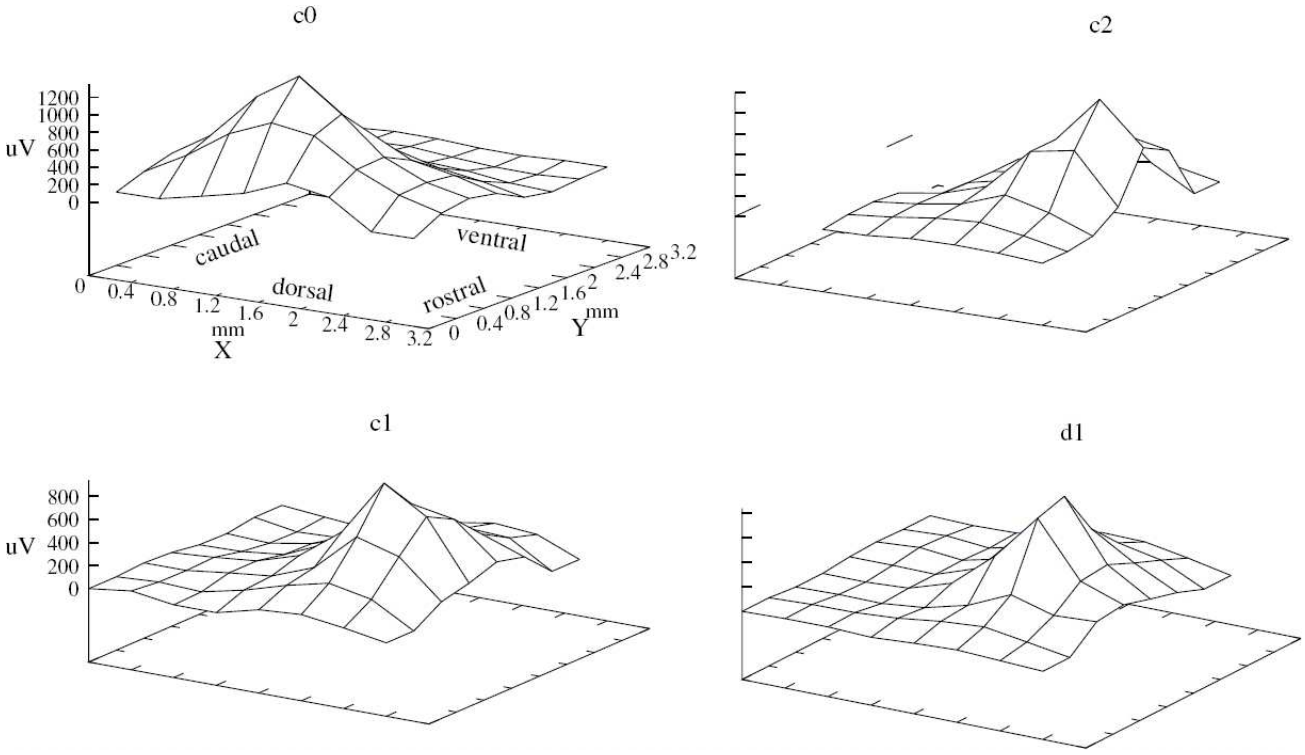
c0
c2
c1
d1
uV
1200
1000
800
600
400
200
0
caudal
dorsal
ventral
rostral
0
0.4
0.8
1.2
1.6
2
2.4
2.8
3.2
mm
X
Y

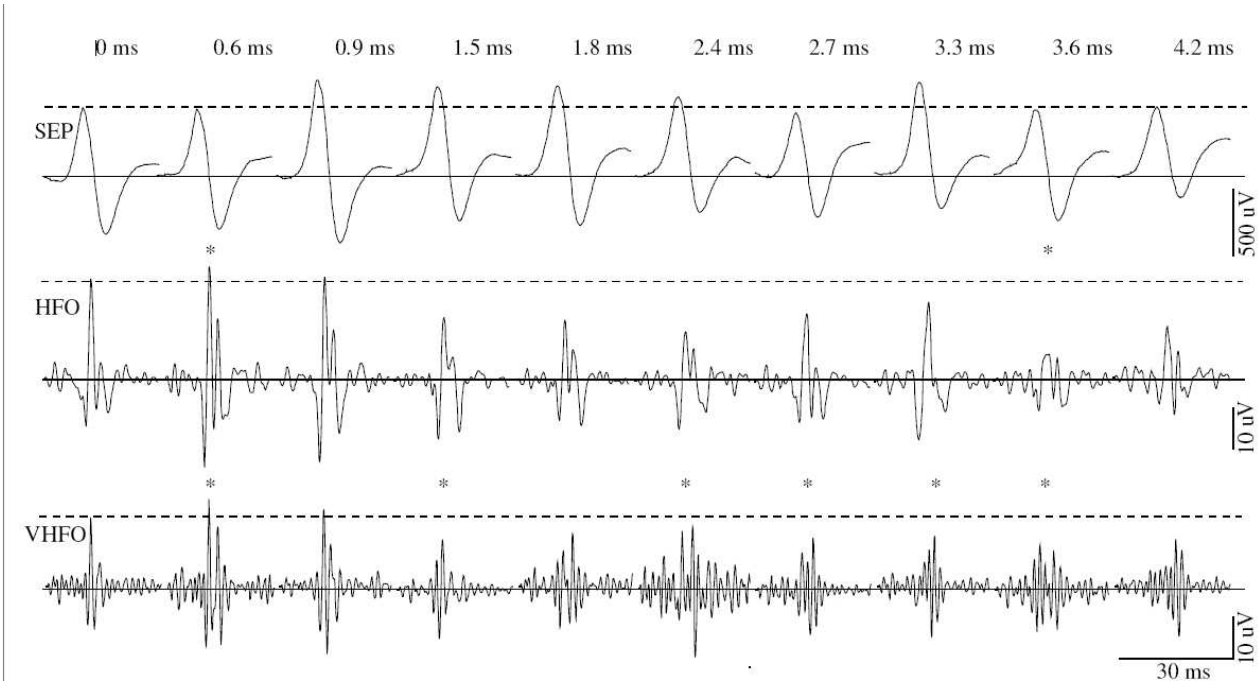
0 ms
0.6 ms
0.9 ms
1.5 ms
1.8 ms
2.4 ms
2.7 ms
3.3 ms
3.6 ms
4.2 ms
SEP
500 uV
HFO
10 uV
VHFO
10 uV
30 ms

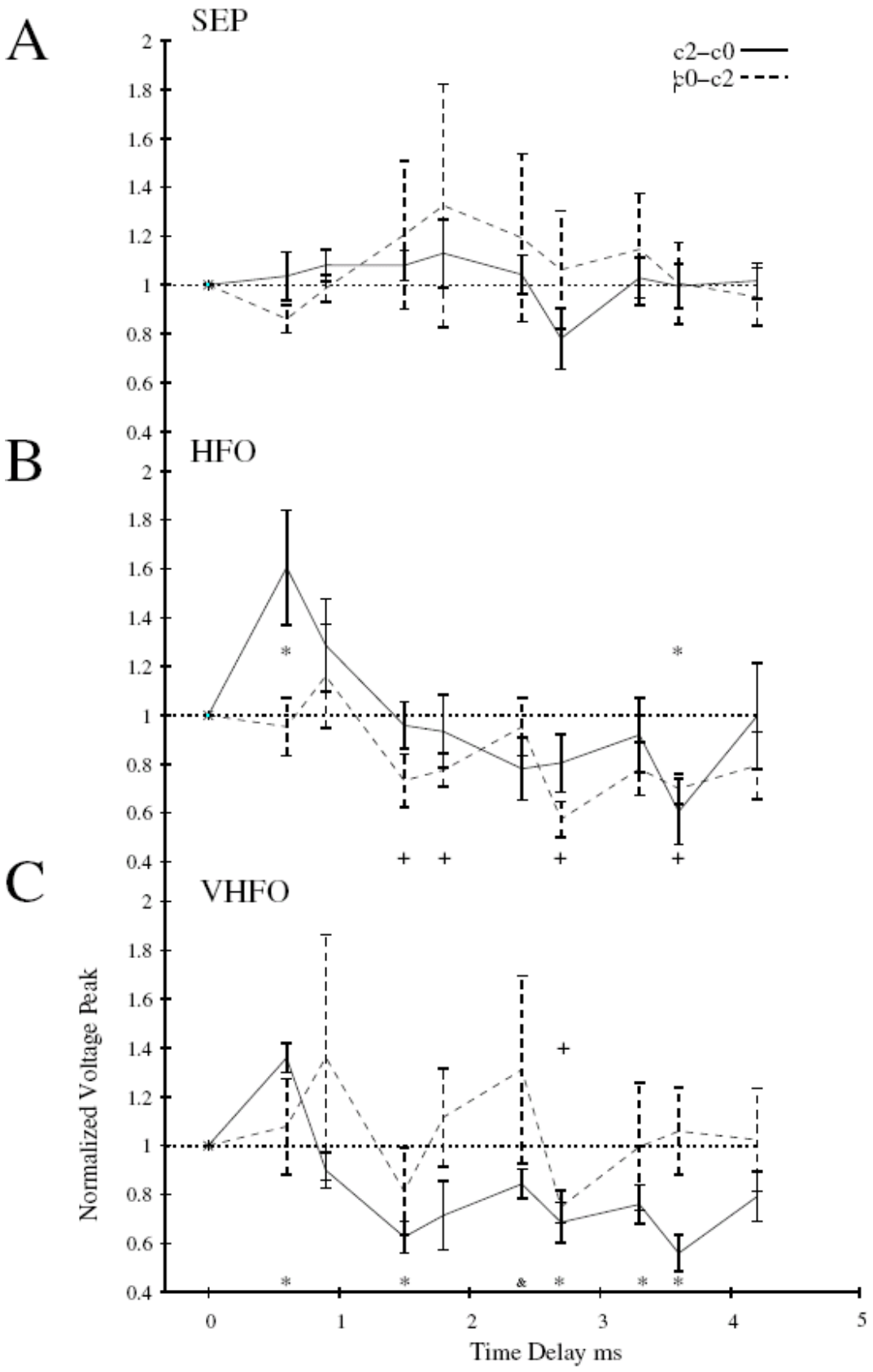
A
SEP
c2–c0
c0–c2
B
HFO
C
VHFO
Normalized Voltage Peak
Time Delay ms

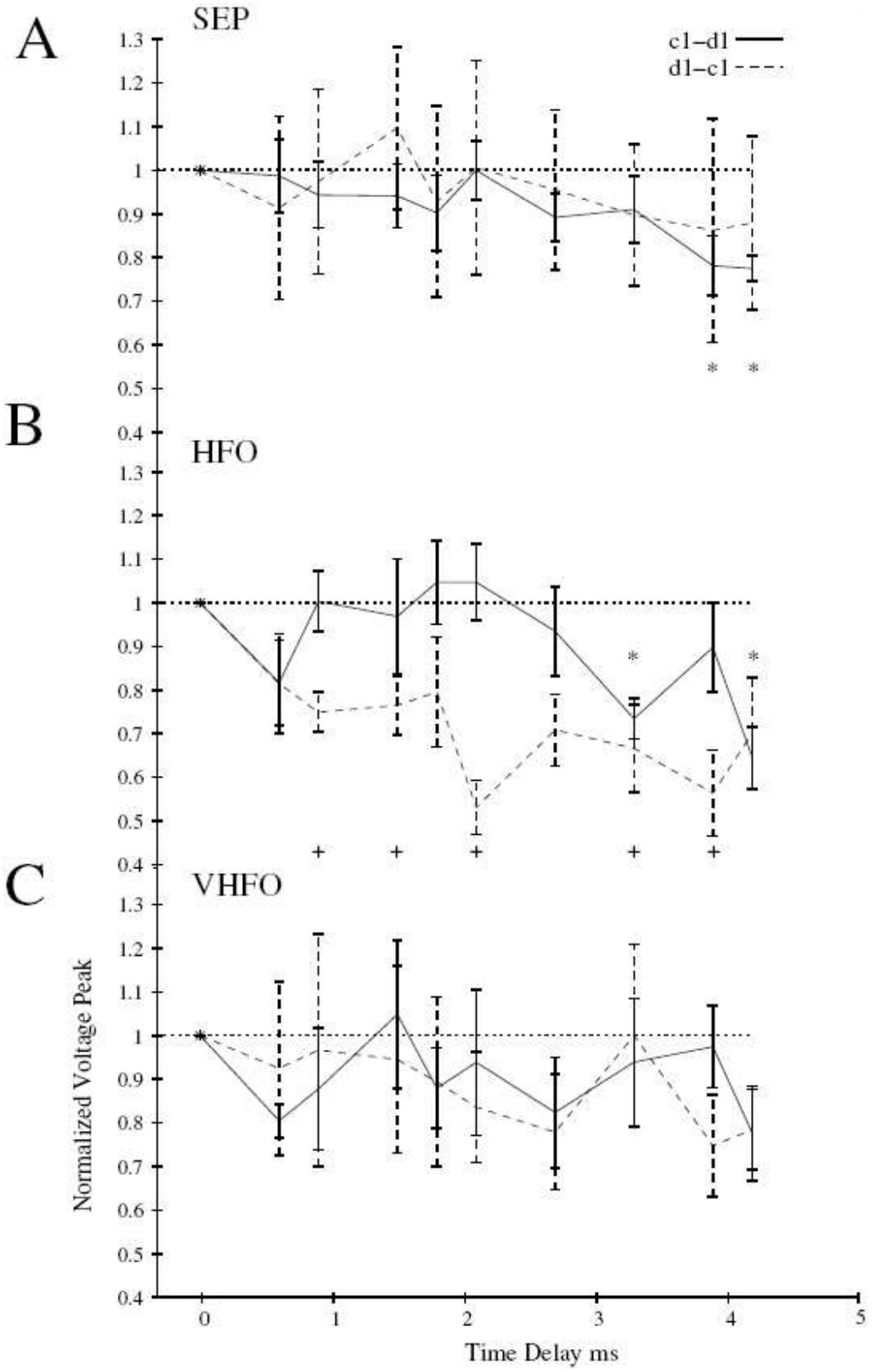
A
SEP
c1–d1
d1–c1
B
HFO
C
VHFO
Normalized Voltage Peak
Time Delay ms

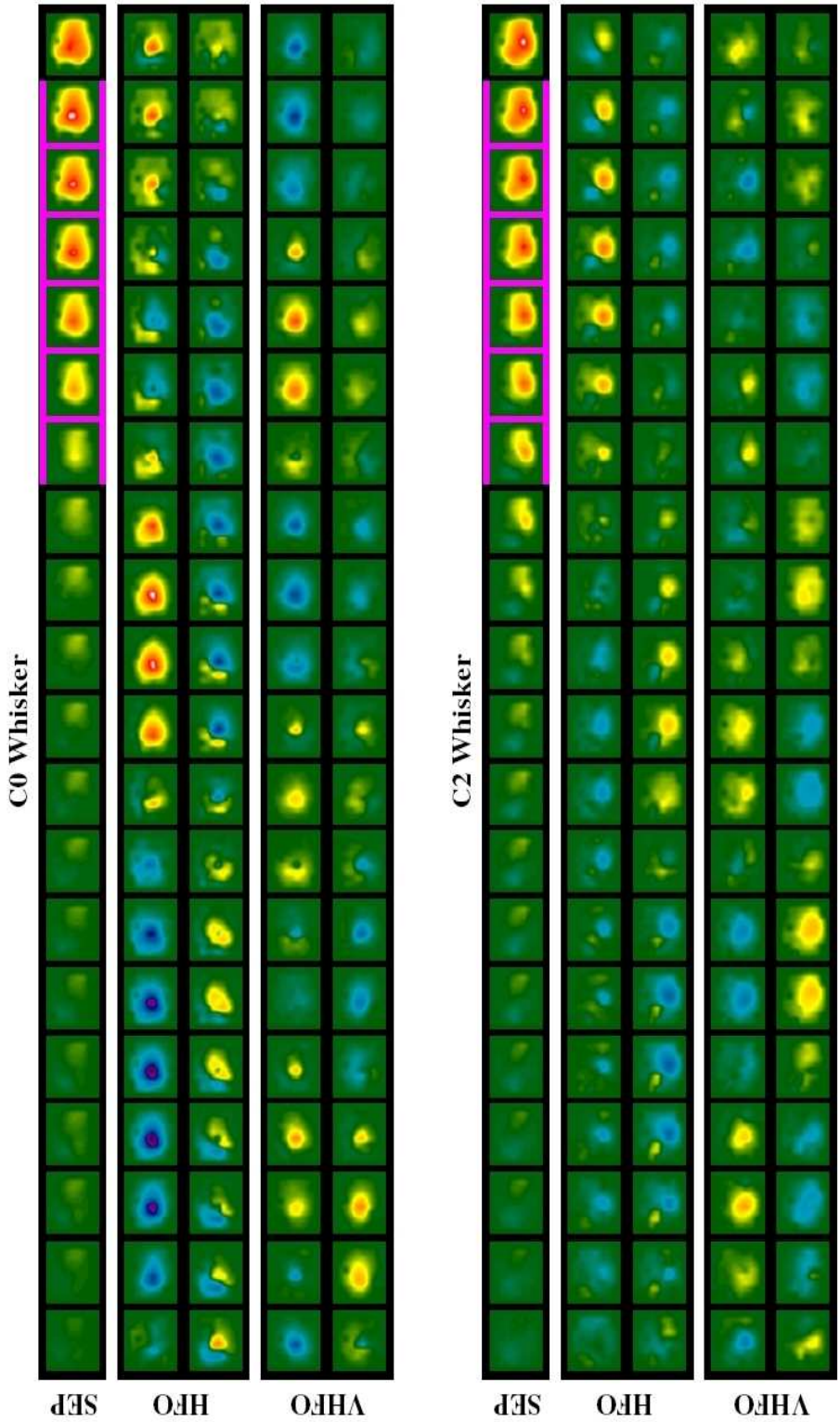
C0 Whisker
C2 Whisker
SEP
HFO
VHFO
SEP
HFO
VHFO

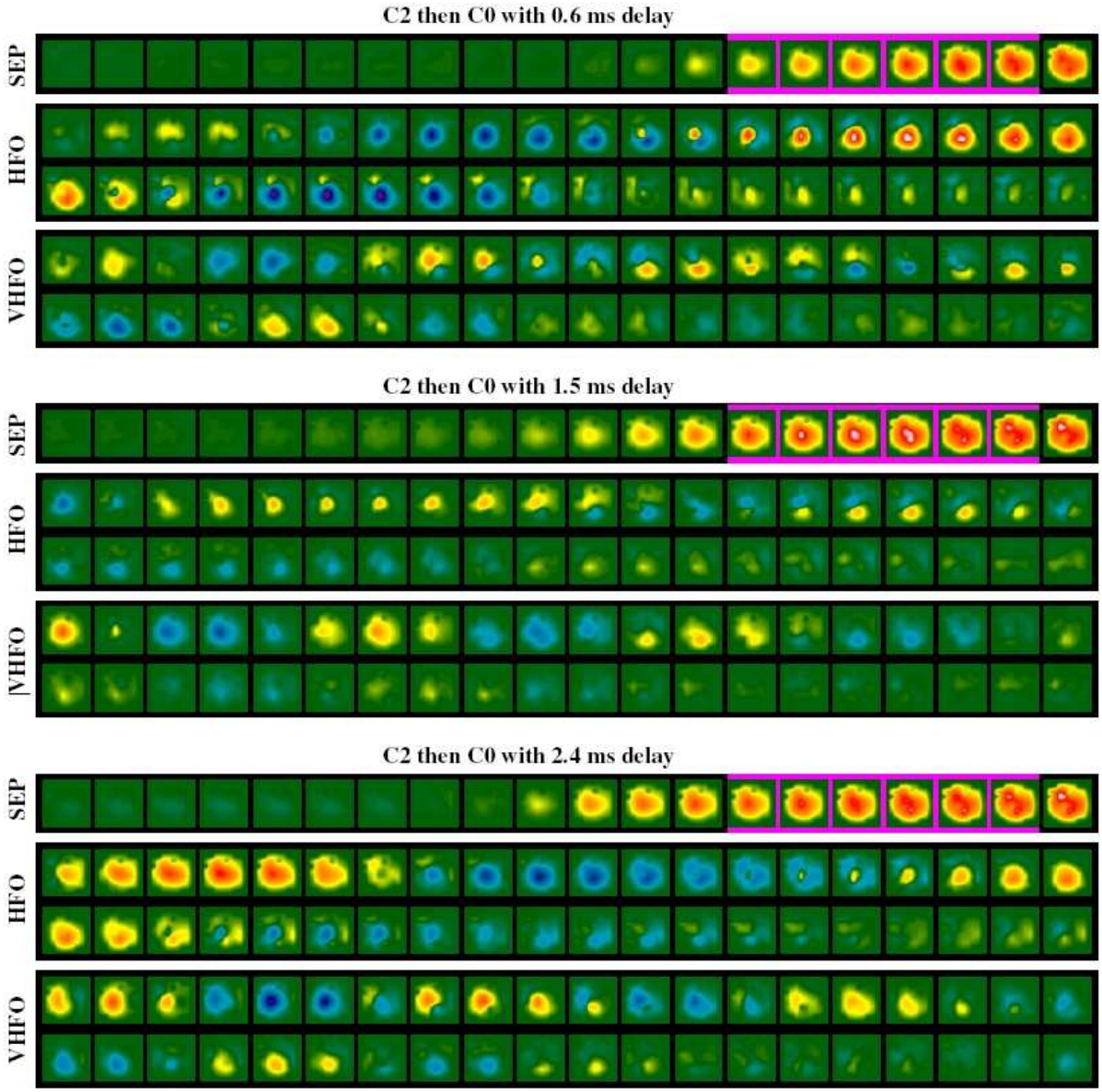
C2 then C0 with 0.6 ms delay
SEP
HFO
VHFO
C2 then C0 with 1.5 ms delay
SEP
HFO
VHFO
C2 then C0 with 2.4 ms delay
SEP
HFO
VHFO

FIGURE LEGENDS

Figure 1. A pictorial diagram of the rat shows the placement of the 64-channel array (E), the screw electrode for recording the EEG and the reference screw (•). B: Bregma; L: Lambda; T: Temporal ridge. EKG was recorded through pins inserted across the chest.

Figure 2. Whisker Barrel Mapping. The somatosensory evoked potential (SEP) across the 64-channel array during whisker stimulation is shown in a two-dimensional (2D) topographical mesh, localizing the corresponding whisker barrel for each of four whiskers c0, c1, c2 and d1.

Figure 3. Averaged signals (n=50) for one animal are displayed from the electrode between whisker barrels stimulated the rostral to caudal sequence at different delays. In the top row of traces, the unfiltered signals reveal the principle 40 Hz SEP component that is not significantly affected by interstimulus delays. When the raw signals were filtered between 200 and 400 Hz, the middle row shows significant supralinear and sublinear effects in peak amplitudes depending on the interstimulus interval indicated with (*). When the raw signals were filtered between 400 to 600 Hz the bottom row shows significant supralinear and sublinear effects with a slightly different pattern.

Figure 4. Plotting the SEP, HFO and VHFO peak amplitude for 6 animals across each interstimulus direction and delay reveals the pattern of wave interaction between two whisker barrels in the same row. Peak SEP P1amplitude (Top panel A) as a function of delay and direction shows no significant differences (Mean +/- SEM). Peak-to-peak HFO amplitude (Middle panel B) as a a function of delay and direction shows supralinear integration at 0.6 msec and sublinear integration at 3.6 msec in the rostral to caudal direction (solid line). Significant differences from the 0 delay condition are marked with (*). In the caudal to rostral direction (dotted line), significant sublinear integration was

found at 1.8, 2.7 and 3.6 msec. Significant differences from 0 delay are marked with plus (+). Peak-to-peak VHFO amplitude (Bottom panel C) as a function of delay and direction shows supralinear integration at 0.6 msec and sublinear integration at 1.5, 2.4, 2.7, 3.3 and 3.6 msec in the rostral to caudal direction (solid line) marked with (*). The amplitude measured at 2.4 ms delay was significantly higher than both 1.5 and 3.6 msec, marked with (&). In the caudal to rostral direction (dotted line), we observed sublinear integration only at 2.7 msec, marked with (+).

Figure 5. Plotting the SEP, HFO and VHFO peak amplitude for 6 animals across each interstimulus direction and delay reveals the pattern of wave interaction between two whisker barrels in the same arc. SEP P1 peak amplitude (Top panel A) as a function of delay and direction shows no significant differences (Mean +/- SEM). B. Peak-to-peak HFO amplitude (Middle panel B) as a function of delay and direction shows sublinear integration at 3.3 and 4.2 msec in the dorsal to ventral direction (solid line). Significant differences from the 0 delay condition are marked with (*). In the ventral to caudal direction (dotted line) significant sublinear integration was found at 0.9, 1.5, 2.1, 2.7, 3.3 and 3.9 msec. Significant differences from 0 delay are marked with plus (+). Peak-to-peak VHFO amplitude (Bottom panel C) as a function of delay and direction shows no significant differences.

Figure 6. Color-coded movies were used to represent SEP and FO voltage levels during stimulation (50 averages) of whisker c0 (upper panel) and c2 (lower panel). Each frame for the SEP is separated by 1 msec in time, beginning 10 ms after the stimulus. Each frame for the HFO and VHFO movies is separated by 0.3 msec. Green colors represent no change in voltage while warmer colors (yellow to red) encode positive voltage deflection (Maximun = white; 500 uV for SEP; 20 uV for HFO and 10 uV for VHFO), cooler colors (blue to purple) encode negative deflection (Minimun = black, 500

uV for SEP; 20 uV for HFO and 10 uV for VHFO).

Figure 7. Color-coded movies were used to represent SEP and FO voltage levels after rotral to caudal asynchronous stimulation (50 averages) at three different delays 0.6 msec (upper panel), 1.5 msec (middle panel) and 2.4 msec (bottom panel). Each frame for the SEP is separated by 1 msec in time, beginning 10 ms after the stimulus. Each frame for the HFO and VHFO movies is separated by 0.3 msec. Green colors represent no change in voltage while warmer colors (yellow to red) encode positive voltage deflection (Maximun = white; 500 uV for SEP; 20 uV for HFO and 10 uV for VHFO), cooler colors (blue to purple) encode negative deflection (Minimun = black, 500 uV for SEP; 20 uV for HFO and 10 uV for VHFO).

Dir		Delay ms	0.6	0.9	1.5	1.8	2.4	2.7	3.3	3.6	4.2	ANOV (F;P)	2 AN vs SEP (F;P)
c2-c0	SEP	Mean	1.04	1.08	1.08	1.13	1.04	0.78	1.03	1	1.02	**0.616 0.778**	
		SEM	0.098	0.064	0.063	0.139	0.08	0.125	0.083	0.092	0.072		
		t_test	0.119	0.115	0.25	0.36	0.27	0.57	0.29	0.35	0.35		
	HFO	Mean	1.61	1.29	0.96	0.93	0.78	0.81	0.92	0.61	1	**3.170 0.004**	0.275 0.601
		SEM	0.235	0.190	0.096	0.150	0.128	0.119	0.152	0.134	0.218		
		t_test	**0.050**	0.193	0.685	0.675	0.149	0.161	0.620	**0.01**	0.68		
	VHFO	Mean	1.36	0.90	0.63	0.71	0.84	0.69	0.76	0.56	0.79	**7.988 <0.000**	**7.568 0.007**
		SEM	0.06	0.07	0.07	0.14	0.06	0.142	0.08	0.07	0.1		
		t_test	**0.002**	0.219	**0.002**	0.10	**0.05**	**0.013**	**0.03**	**<0.00**	0.09		
c0-c2	SEP	Mean	0.99	0.98	1.29	1.32	1.28	1.13	1.13	1.02	0.96	**0.353 0.952**	
		SEM	0.073	0.061	0.289	0.491	0.322	0.199	0.231	0.151	0.112		
		t_test	0.465	0.475	0.15	0.25	0.19	0.27	0.28	0.35	0.37		
	HFO	Mean	0.95	1.16	0.73	0.78	0.96	0.57	0.78	0.7	0.79	**2.276 0.032**	**10.151 0.002**
		SEM	0.119	0.212	0.109	0.067	0.121	0.073	0.108	0.061	0.139		
		t_test	0.711	0.484	0.06	**0.02**	0.771	**0.002**	0.1	**0.003**	0.09		
	VHFO	Mean	1.08	1.36	0.81	1.12	1.31	0.75	1	1.06	1.02	**0.543 0.836**	0.277 0.6
		SEM	0.196	0.503	0.177	0.201	0.385	0.066	0.261	0.178	0.210		
		t_test	0.705	0.505	0.34	0.59	0.46	0.01	0.99	0.75	0.91		

Table 1. Voltage Peak Amplitude mean and SEM values for SEP, HFO and VHFO in the rostral to caudal sequence of stimulation c2-c0 and in the caudal to rostral direction c0-c2. One way ANOVA with delay as a factor, and Two way ANOVA with delay and wave types as factor for every sequence of stimulation.

Dir		Delay ms	0.6	0.9	1.5	1.8	2.1	2.7	3.3	3.9	4.2	ANOV (F;P)	2 AN vs SEP (F;P)
c1-d1	SEP	Mean	0.99	0.94	0.94	0.9	1	0.89	0.91	0.78	0.77	**1.478 0.182**	
		SEM	0.083	0.076	0.073	0.087	0.068	0.054	0.076	0.069	0.03		
		t_test	0.882	0.488	0.456	0.311	0.993	0.104	0.291	0.025	0.001		
	HFO	Mean	0.82	1	0.97	1.05	1.05	0.93	0.73	0.9	0.65	**2.445 0.022**	0.009 0.924
		SEM	0.24	0.17	0.32	0.24	0.21	0.25	0.11	0.25	0.17		
		t_test	0.118	0.962	0.825	0.644	0.611	0.420	**0.002**	0.364	**0.004**		
	VHFO	Mean	0.8	0.88	1.05	0.88	0.94	0.82	0.94	0.97	0.78	**0.551 0.830**	0.025 0.874
		SEM	0.09	0.34	0.41	0.23	0.41	0.31	0.36	0.23	0.26		
		t_test	0.004	0.421	0.785	0.246	0.729	0.224	0.694	0.796	0.093		
d1-c1	SEP	Mean	0.91	0.97	1.1	0.93	1.01	0.96	0.9	0.86	0.88	**0.126 0.999**	
		SEM	0.210	0.212	0.186	0.219	0.246	0.183	0.162	0.256	0.199		
		t_test	0.697	0.907	0.624	0.755	0.982	0.816	0.554	0.614	0.571		
	HFO	Mean	0.82	0.75	0.77	0.8	0.53	0.71	0.67	0.56	0.7	**2.142 0.043**	**10.224 0.002**
		SEM	0.28	0.11	0.17	0.31	0.15	0.2	0.25	0.24	0.31		
		t_test	0.165	**0.003**	**0.018**	0.166	**0.001**	**0.017**	**0.021**	**0.007**	0.066		
	VHFO	Mean	0.92	0.97	0.95	0.89	0.84	0.78	1	0.75	0.78	**0.307 0.969**	0.583 0.447
		SEM	0.49	0.65	0.53	0.48	0.31	0.32	0.51	0.29	0.23		
		t_test	0.720	0.905	0.809	0.610	0.254	0.155	1.000	0.082	0.067		

Table 2. Voltage Peak Amplitude mean and SEM values for SEP, HFO and VHFO in the dorsal to ventral sequence of stimulation c1-d1 and in the ventral to dorsal direction d1-c1. One way ANOVA with delay as factor, and Two way ANOVA with delay and wave types as factor for every sequence of stimulation.